Analytical Methods

ROYAL SOCIETY OF CHEMISTRY

PAPER

View Article Online
View Journal | View Issue

Cite this: *Anal. Methods*, 2024, **16**, 91

Electrokinetic focusing of SARS-CoV-2 spike protein *via* ion concentration polarization in a paper-based lateral flow assay†

Kira L. Rahn, Sommer Y. Osman, Quinlan G. Pollak and Robbyn K. Anand *

The COVID-19 pandemic highlighted the importance of designing sensitive and selective point-of-care (POC) diagnostic sensors for early and rapid detection of infection. Paper-based lateral flow assays (LFAs) are easy to use, inexpensive, and rapid, but they lack sensitivity. Preconcentration techniques can improve the sensitivity of LFAs by increasing the local concentration of the analyte before detection. Here, ion concentration polarization (ICP) is used to focus the analyte, SARS-CoV-2 Spike protein (S-protein), directly over a test line composed of angiotensin converting enzyme 2 (ACE2) capture probes. ICP is the enrichment and depletion of electrolyte ions at opposing ends of an ion-selective membrane under a voltage bias. The ion depleted zone (IDZ) establishes a steep gradient in electric field strength along its boundary. Enrichment of charged species (such as a biomolecule analyte) occurs at an axial location along this electric field gradient in the presence of a fluid flow that counteracts migration of those species – a phenomenon called ICP focusing. In this paper, running buffer composition and pretreatment solutions for ICP focusing in a paper-based LFA are evaluated, and the method of voltage application for ICP-enrichment is optimized. With a power consumption of 1.8 mW, S-protein is concentrated by a factor of 21-fold, leading to a 2.9-fold increase in the signal from the LFA compared to a LFA without ICP-enrichment. The described ICP-enhanced LFA is significant because the preconcentration strategy is amenable to POC applications and can be applied to existing LFAs for improvement in sensitivity.

Received 15th June 2023
Accepted 22nd November 2023

DOI: 10.1039/d3ay00990d

rsc.li/methods

1. Introduction

In this paper, we describe a method to increase the sensitivity of a lateral flow assay (LFA) for SARS-CoV-2 Spike protein (S-protein) using an electrokinetic focusing technique, ion concentration polarization (ICP). To achieve this result, we use ICP to enrich the S-protein in the sample directly over an angiotensin converting enzyme 2 (ACE2) capture probe and keep it in place to allow for improved binding of the antigen to the test line. The results of this study are important for two reasons. First, we discuss important parameters for designing a paper-based assay that is compatible with ICP and identify an appropriate pretreatment solution and running buffer. Second, we demonstrate a configuration and method that allow for enrichment of the S-protein in a consistent location in the LFA to ensure binding of the antigen to the test line. Importantly, the methods discussed below are not unique to the S-protein/ACE2 pair and can be combined with other paper-based LFAs for improvements in sensitivity.

The need for increased sensitivity of selective point of care (POC) biosensors has been made emergent by the COVID-19 pandemic.[1–4] The virus is contagious, by both symptomatic and asymptomatic individuals. Testing methods that facilitate early diagnosis are required to administer early treatment for at-risk individuals, decrease the spread of the virus, and track case rates for resource allocation. An ideal diagnostic test would be rapid, inexpensive, sensitive enough for early diagnosis, and not require trained personnel.[4–6] Amplification strategies, like reverse transcription polymerase chain reaction (RT-PCR), are extremely sensitive and selective, however they require long times, expensive equipment, and trained technicians to perform.[1,4]

LFAs are ideal POC sensors for rapid and inexpensive diagnosis, however they lack sensitivity.[1,5,6] In a LFA, the antigen-containing sample is flowed across a paper strip containing a test line composed of an immobilized capture probe that selectively binds to the antigen.[6,7] A transduction element is present in the assay to indicate presence or absence of the analyte. For example, a detector antibody that binds to the antigen and is conjugated to a Au nanoparticle can be added to the assay for colorimetric detection. The typical sensitivity of a LFA is on the order of 10 μM.[1] Increasing the sensitivity LFAs is important so that infectious diseases, like COVID-19, can be

Department of Chemistry, Iowa State University, 1605 Gilman Hall, 2415 Osborn Drive, Ames, IA 50011-1021, USA. E-mail: rkanand@iastate.edu

† Electronic supplementary information (ESI) available. See DOI: https://doi.org/10.1039/d3ay00990d

diagnosed earlier in the disease progression. There are three main strategies for increasing the sensitivity of a LFA: develop higher affinity biorecognition elements, improve transduction techniques, and preconcentrate or amplify the antigen.[1,5,7,8] Preconcentration methods are attractive because these techniques can be applied to any LFA.

Existing strategies for improving the sensitivity of LFAs with preconcentration include the use of isotactophoresis,[8] magnetic fields,[9] two-phase micellar systems,[10] and pressure.[11] While these methods improve the sensitivity of LFAs, they require several user steps that may add to user-to-user reproducibility issues. ICP is an attractive method for further improving the sensitivity of LFAs because beyond sample addition, the only user-required step is to push a button to turn on a power source (such as a battery). Additionally, the enriched plug can be held directly over the test line for an extended period, allowing for improved binding of the antigen to the capture probe.

ICP is an electrokinetic technique where background electrolyte ions are simultaneously depleted and enriched at opposing ends of an ion-selective structure in the presence of an electric field to form an ion depleted zone (IDZ) and ion enriched zone (IEZ).[12–14] A local electric field enhancement is formed within the IDZ, and charged analytes are focused along the electric field gradient at the boundary of the IDZ when electro-migratory and convective velocities are balanced. Several groups have already demonstrated the use of ICP focusing in a paper-based device.[15–21] Han and coworkers patterned Nafion, an ion selective membrane, on tape and showed that 300-fold preconcentration of a protein could be achieved in a cellulose strip.[15] Frequently, the voltage to induce ICP is applied between two electrodes, one in the sample inlet and one in contact with the cation selective membrane.[15,16] Kwak and co-workers showed, in a microfluidic channel, that by applying the voltage directly to two Nafion membranes, improved preconcentration was achieved and the location of the focused plug remained more stationary.[22] Kim and co-workers also used this double-gate design to preconcentrate β human chorionic gonadotropin (β-HCG), the protein detected in pregnancy LFAs, using a battery-operated device.[17] Notably, preconcentration of the target was performed before the assay and off-strip, instead of directly over the test line. After preconcentration, Kim and co-workers introduced the enriched plug to the LFA strip and allowed the target to flow downstream for β-HCG detection. While they were able to preconcentrate the antigen by a factor of 25, the overall improvement to sensitivity remained 2.69-fold. We hypothesize that enriching the antigen off-strip and subsequently flowing the focused plug onto the LFA led to diffusional broadening and a decreased interaction time between the antigen and the antibody. Further work from this group improved upon this design by incorporation of rolled paper disks for the anode, cathode, and collection area.[23] By application of 150 V, SARS-CoV-2 IgG from serum was preconcentrated and then added to a commercial LFA with a 32-fold improvement in the LOD. Recently, an ICP-integrated LFA has been demonstrated by enriching SARS-CoV-2 nucleocapsid protein directly over the commercial test line to achieve an enrichment factor greater than 10.[24] Most interestingly, the addition of stacked paper layers between the cation exchange membrane and the paper strip inhibited pH changes that can occur when the acidic Nafion membrane is in direct contact with the LFA.

Here, we demonstrate the ICP-driven enrichment of an antigen directly over the capture probes in a LFA that results in binding of the antigen-probe pair. A Pluronic solution is identified as a low-conductivity solution compatible with ICP that also works as a pretreatment solution to attenuate non-specific adsorption of the antigen in the nitrocellulose membrane. Similarly, HEPES buffer is identified as an ICP and biocompatible buffer due to its low conductivity and buffering range. We optimize the device configuration to obtain a reproducible and stationary enrichment location that spans the width of the test line in the LFA. We quantify the impact of magnitude of voltage application and time of voltage application on the binding of the focused antigen to the capture probe. We demonstrate that the ICP-enhanced LFA improves the sensitivity by a factor of 2.9. Combined, these results demonstrate a new platform for improving the sensitivity of LFAs with ICP focusing.

2. Theoretical background

2.1 Binding kinetics in a LFA

The binding of the antigen to the capture probe is a reversible process that can be modeled as a second order reaction with an equilibrium dissociation constant, K_D, equal to the ratio of dissociation (k_d) and association (k_a) rate constants: $K_D = \frac{k_d}{k_a}$.[8,25,26] The Damköhler number (Da) is the ratio between maximum reaction and diffusion rates and is often used to determine if the reaction is in a mass transport limited or kinetically limited regime.[8,25,26] If Da $\gg$ 1, then the rate is limited by mass transport (diffusion and convection), while if Da $\ll$ 1, the rate is limited by kinetics. For a LFA in nitrocellulose, $\mathrm{Da} = \frac{k_a \tilde{C}_{p0} d}{D}$ where $\tilde{C}_{p0}$ is the surface concentration of capture probe, d is the nitrocellulose pore radius, and D is the diffusivity of the antigen in the nitrocellulose membrane.[8] Typically d is the channel height, but since the channel is composed of porous paper (nitrocellulose membrane), the pore radius was chosen as the characteristic length for diffusion of the proteins.[8] For our assay in the absence of ICP, we estimate Da to be on the order of 10^{-4} indicating that the assay is kinetically limited (see the ESI† for more details on this calculation).

If we assume perfect mixing and that convection and diffusion supply the antigen to the capture probe faster than the reaction kinetics (*i.e.*, we are in a kinetically limited case), and the concentration of the antigen near the capture probes is approximately equal to the concentration of the antigen added, then the fraction (h_{lfa}) of the surface concentrations of bound capture probes ($\tilde{C}_b$) to $\tilde{C}_{p0}$ can be estimated by eqn (1):[8,25,26]

$$h_{lfa} = \frac{\tilde{C}_b}{\tilde{C}_{p0}} = \frac{C_0^*}{1 + C_0^*}\left(1 - \exp\left(-\left(C_0^* + 1\right)k_d t\right)\right) \quad (1)$$

where C_0^* is the initial molar concentration of the antigen in the immediate vicinity of the capture probes normalized by K_D. See the ESI† for a derivation of eqn (1).

For an interpretation of the relationship in eqn (1), it is useful to consider the assay at two concentrations of antigen added to the assay. When a 1.3 nM solution of S-protein is added to the assay, 99% of the capture probes that will bind to the antigen will be bound within 12 min. The fraction of capture probes that will bind is approximately 0.4% of the total probes. On the other hand, when a 10-fold more concentrated solution of antigen is added (13 nM solution of S-protein) to the assay, 4% of the total probes will bind, with 99% of those probes binding within 11.6 min. In other words, the 10-fold increase in concentration of antigen (1.3–13 nM) should yield an approximately 10-fold increase in percent of bound capture probes. In the 13 nM case, it takes 1.7 min for 2% of the probes to bind and 3.5 min for 3% of the probes to bind. These cases highlight the importance of (1) increasing the local concentration of the antigen over the capture probes and (2) allowing sufficient time for the complex formation to occur so that a higher proportion of capture probes will be bound to the antigen at equilibrium.

2.2 ICP in a paper-based device

In our ICP-enhanced paper-based LFA, depicted in Scheme 1, a cellulose pad serves as the sample inlet. The sample pad is in contact with a nitrocellulose membrane where the capture probe has been deposited and focusing occurs. The sample is wicked through the nitrocellulose membrane to a fan-shaped piece of filter paper, which acts as a waste pad. The fan shape is used to maintain a more constant capillary flow rate.[27] The voltage for ICP is applied to two AgCl ink electrodes that are patterned with Nafion, which is the ion-selective structure. Nafion is a membrane with negatively charged pores that electrostatically exclude anions, allowing only cations to pass through the membrane.

The mechanism for ICP in our LFA is depicted in Scheme 2. As shown in Scheme 2a, upon addition of the sample to the sample pad, the background electrolyte initially spreads evenly through the nitrocellulose membrane. When voltage is applied, the cations (blue circles) migrate towards the cathode, travel through the cation-selective membrane, and are consumed or balanced by electrochemical reactions. Meanwhile, anions (red circles) migrate towards the anode and accumulate around the cation-selective membrane. Cations are produced by electrochemical reactions at the anode and accumulate near the anions to satisfy charge neutrality. In time, an IEZ is formed near the anode, while an IDZ is formed near the cathode. A steep electric field gradient exists between the IDZ and IEZ, depicted in Scheme 2b, where the analyte (green circle) is enriched in the position where its electrophoretic (v_{el}) and convective (v_c) velocities are balanced. The test line of the LFA is aligned at the position where focusing occurs (Scheme 2c).

Current voltage curves (CVCs) are often obtained for ICP devices to characterize the system.[19,20] In a CVC, the voltage applied to the device is increased as the current is measured. There are three regions in a CVC: the ohmic region, the limiting region, and the over-limiting region. At low voltages, the IDZ and IEZ have not yet formed. The Nafion-coated electrodes and sample-soaked nitrocellulose membrane act as a resistor. Therefore, by Ohm's law, the current is equal to the voltage applied divided by the resistance of the device. The slope of the CVC is linear and constant in the ohmic region. As the voltage

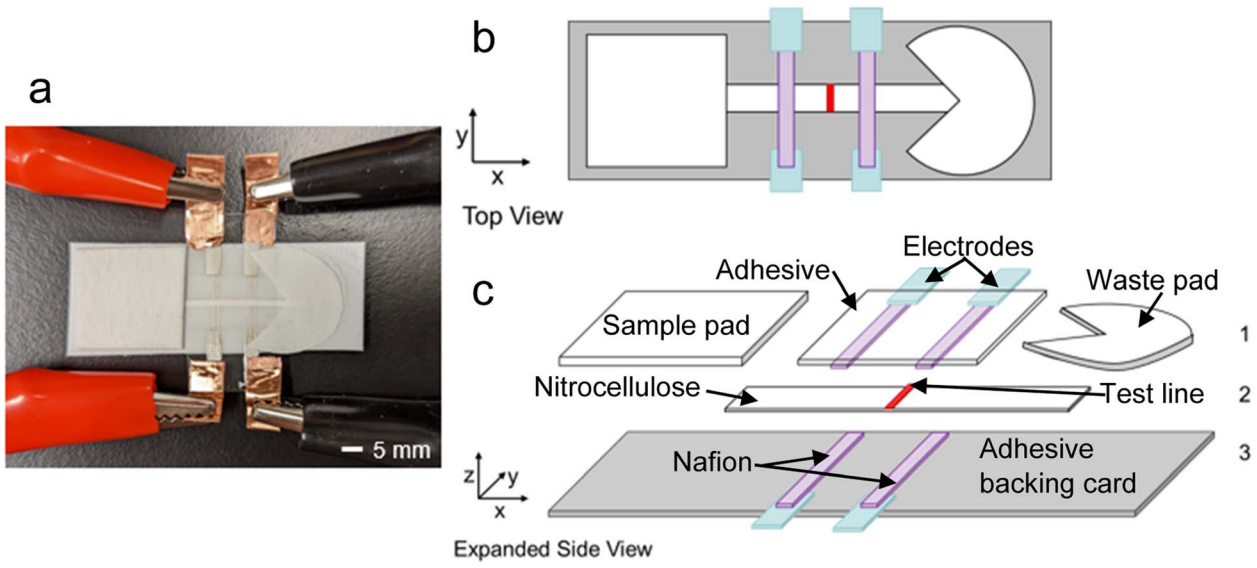

Scheme 1 Device design for the ICP-enhanced LFA.[a] (a) Image of the assembled ICP-enhanced LFA. (b) Top view schematic of the ICP-enhanced LFA. (c) Expanded side view schematic of the ICP enhanced LFA. Layer 1, from left to right: cellulose sample pad, two cation-selective membranes (Nafion, purple) painted on microfluidic diagnostic tape in contact with two AgCl ink electrodes (light blue), fan-shaped filter paper waste pad. Layer 2: nitrocellulose membrane painted with a test line (red). Layer 3: two cation-selective membranes (Nafion, purple) painted on adhesive backing card (grey) in contact with two AgCl ink electrodes (light blue).

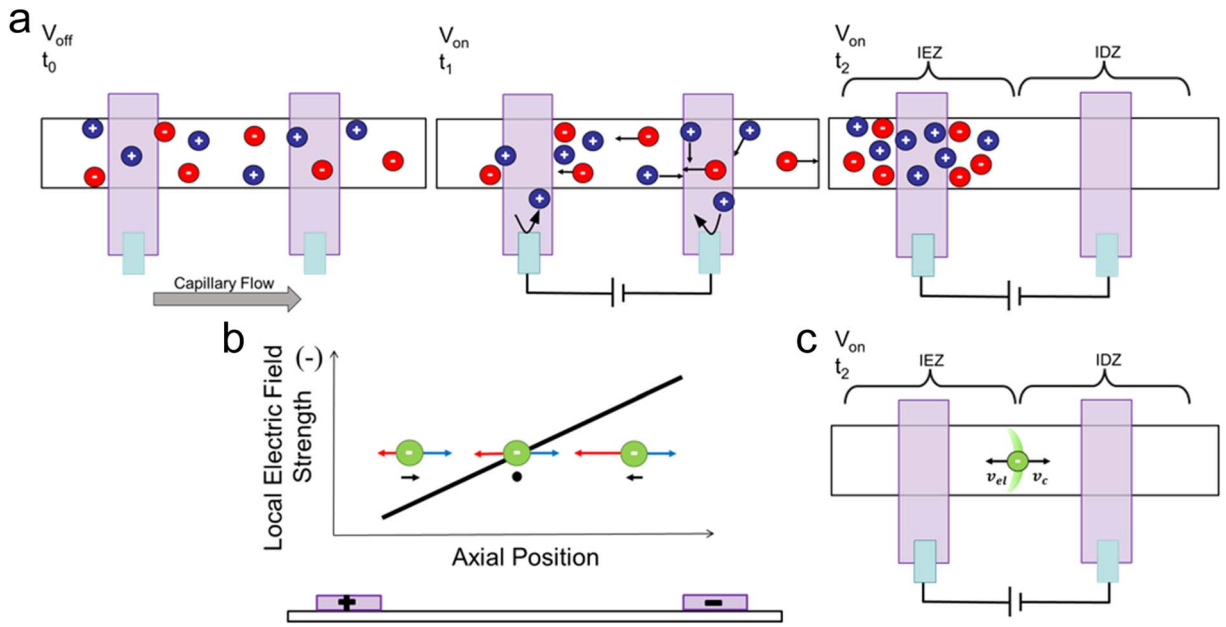

Scheme 2 Depiction of ICP in a LFA including (a) redistribution of ions in the paper strip under an applied voltage and capillary flow, (b) counterflow focusing of an anionic analyte in the resulting electric field gradient, and (c) locations of the IEZ, IDZ and focused analyte plug.

increases further, the IDZ forms. This region of the CVC is called the limiting region because the resistance is increasing due to the depletion of ions, limiting the current through the device. Increasing the voltage even higher can lead to the formation of electroconvective vortices that allow the IDZ and IEZ to mix. This mixing allows ions to pass through the depletion zone, so the current can again increase. In cellulose-based devices, another region of limiting-current can be observed because the size of the electroconvective vortices is confined by the fibers in the cellulose.[20]

3. Experimental section

3.1 Materials

AgCl ink was purchased from Nagase ChemTeX American Corporation (CI-4002, Delaware, OH). Backing cards were purchased from DCNovations (Carlsbad, CA), microfluidic diagnostic tape was purchased from 3M (9964, St. Paul, MN), nitrocellulose membranes with 0.45 μm pore size were purchased from Thermo Scientific (Waltham, MA), and cellulose fiber sample pads were purchased from Millipore Sigma (Burlington, MA). Nafion perfluorinated resin solution, 20 wt%, Bis-Tris propane, and Pluronic F-127 were purchased from Sigma-Aldrich (St. Louis, MO). Recombinant Human ACE2 protein with an mFc Tag (Cat# 10108-H05H) and SARS-CoV-2 (2019-nCoV) Spike S1-His Recombinant Protein (Cat# 40591-V08H) were purchased from Sino Biological (Beijing, China). Tween-20, Whatman filter paper Grade 1, and Tris·HCl (1.0 M solution), were purchased from Fisher Scientific (Waltham, MA). HEPES was purchased from MP Biomedicals (Pittsburgh, PA). Texas Red and Alexa Fluor-488 Lightening Link Conjugation kits were purchased from Abcam (Eugene, OR). BODIPY^{2-} (4,4-difluoro-1,3,5,7,8-pentamethyl-4-bora-3*a*,4*a*-diaza-*s*-indacene-2,6-disulfonic) was purchased from Molecular Probes (Eugene, OR). All solutions were diluted with double deionized water (18.2 MΩ cm, Sartorius Arium Pro, Göttingen, Germany).

3.2 Nafion-coated electrodes

AgCl ink was painted onto transparency films using a sponge brush onto a laser-cut stencil. For the bottom electrodes (under the LFA paper strip), the AgCl electrodes were cut then attached to the adhesive side of the backing card. For the top electrodes, the AgCl electrodes were attached to the adhesive side of the microfluidic diagnostic tape. Nafion perfluorinated resin solution was painted on the electrodes and adhesives using a modified automated LFA reagent dispenser. The dispenser (purchased from Claremont Bio, Upland, CA) was modified by enlarging the holes on the needle holder to fit larger PTFE tubing (1.0 mm inner diameter). Nafion was dispensed at a rate of 8.0 μL s^{-1} with a dispenser voltage of 3.0 V. Nafion membranes were 1.0 mm wide with a 5.0 mm gap between the inner edges of the anodic and cathodic membranes. After dispensing, the membranes were baked at 65 °C for 10 min, then cooled to room temperature before soaking in ultrapure water overnight. The Nafion membranes were soaked to hydrate the membranes to increase conductivity.

3.3 Conjugating proteins with fluorescent dyes

ACE2 and S-protein were modified with red and green fluorescent dyes, respectively. Directions from the Lightning Link Conjugation Kits were followed, with the exception of the starting mass of protein added to the kit. The kits are designed for conjugating antibodies, and since both proteins have smaller molecular weights (110 kDa for ACE2 and 76.5 kDa for S-protein) than antibodies (~150 kDa), smaller masses of protein were added to

the 100 μg conjugation kits. For conjugating ACE2 to Texas Red, 136.4 μL of ultrapure water was added to the 100.0 μg vial of ACE2 from Sino Biological, and 100.0 μL of that solution (with a concentration of 73.3 μg of ACE2 per 100.0 μL) was mixed with 10 μL of the Modifier reagent from the kit. The solution was mixed with the dye and allowed to incubate for 15 min in the dark. Then, 10 μL of quencher reagent was added to the dye solution and allowed to incubate for 5 min before 0.05% NaN_3 was added to the stock solution. Solutions were stored at 4 °C until used. For S-protein, 200.0 μL of ultrapure water was added to a vial of 100.0 μg of the protein, and 100.0 μL of that solution (with a concentration of 50.0 μg S-protein per 100.0 μL) was used with the AF-488 Conjugation kit as described for the Texas Red Conjugation kit above. The final concentration of ACE2 was 0.59 μg μL^{-1} and 0.40 μg μL^{-1} for S-protein.

3.4 Nitrocellulose membranes

For nitrocellulose membranes with test lines, ACE2 conjugated with Texas-Red dye was deposited on the nitrocellulose using the LFA reagent dispenser. A flow rate of 0.88 μL s^{-1} was used to dispense the solution, with a headspeed of 17.5 mm s^{-1}. The ACE2 solution was dispensed on the nitrocellulose membrane for a total of 4 times to deposit 0.118 μg mm^{-1}. The nitrocellulose membrane was dried at room temperature for 1 h, then pretreated with 1.0 mM Pluronic F-127 solution. The pretreated nitrocellulose membranes were allowed to dry at room temperature overnight before use. The strips were cut with a guillotine cutter into 25.0 mm long strips, with widths as described in the *Results and discussion* section.

3.5 Device assembly

Cellulose sample pads were pretreated with the 1.0 mM Pluronic F-127 solution and dried at 65 °C for 2 h before use. Whatman filter paper waste pads were cut in a fan shape so that solution flow was consistent. For a LFA without ICP-enrichment, the nitrocellulose membranes (described above) were placed on the adhesive back card. Sample and waste pads were adhered to the backing card overlapping the nitrocellulose membrane. Microfluidic diagnostic tape was sealed on top of the exposed nitrocellulose membrane.

For LFAs with ICP-enrichment, the backing card and microfluidic diagnostic tape with Nafion-coated electrodes described above were used. First, the Nafion-coated electrodes were dried by blotting on a lint-free wipe. Cu tape was attached to the AgCl electrodes to connect the device to a power supply. Then, the nitrocellulose membrane was aligned so there were 5.0 mm between the membrane and the AgCl electrodes. The Nafion-coated electrodes on the diagnostic tape were aligned on top of the nitrocellulose membrane and backing card and sealed. Sample and waste pads were attached to the backing card, overlapping the nitrocellulose membrane.

The assembled devices were used immediately. A pipette was used to deliver 300 μL of the sample solution (composed of the analyte, the buffer, and 0.05% Tween-20) to the sample pad. If ICP-enrichment was performed, the voltage was turned on immediately after the solution had wicked across both anodic and cathodic Nafion membranes. The fluorescence intensity was monitored with a SMZ800N stereoscope (Nikon Industries, New York, NY) equipped with a Sola Lumencor Light engine (Lumencor, Beaverton, OR) and Photometrics Cool Snap Dyno camera (Tucson, Arizona).

3.6 Data analysis

Fluorescence micrographs were exported as TIF files, and the average fluorescence intensity of the region of interest (the entire nitrocellulose membrane between the two Nafion membranes or the area containing the test line) was calculated using a code implemented in MATLAB. All values were background subtracted by the average fluorescence intensity of the dry nitrocellulose membrane.

4. Results and discussion

4.1 Incorporating Nafion-coated electrodes into a paper-based device

A double-gate design was determined as the most favorable configuration to induce ICP preconcentration because it has been demonstrated that the location and intensity of the enriched plug is more stable and higher in a double-gate design *vs.* a single-gate design.[22] In a single-gate design, the IDZ can propagate upstream, allowing the enriched plug to continuously move upstream as well.[22] For initial characterization, an anionic green-fluorescent dye, $BODIPY^{2-}$, was used as the analyte. Tris buffer was used as the running buffer because it was been previously incorporated with the enrichment of proteins *via* ICP focusing. The surfactant Tween-20 was added to the running buffer because it can lyse viruses, and therefore, it was included to prepare for future studies that will address clinical samples.[28] However, this concentration has since been shown to not effectively lyse SARS-CoV-2.[29]

Our first challenge in developing an ICP-enhanced LFA was determining the best way to establish contact between the Nafion-coated electrodes and the nitrocellulose membrane. We attempted to use magnets and Scotch double-sided tape to attach Nafion-coated AgCl electrodes that were painted on transparency film to the top on the LFA (see Fig. S1†). While enrichment occurred, we realized that the contact between the Nafion and the nitrocellulose membrane would be improved if the Nafion were painted on an adhesive that could stick directly to the nitrocellulose membrane, and not just the tape around it (see Fig. S2†). Therefore, we used the microfluidic diagnostic tape as the backing for the Nafion-coated electrodes and attached it and the sample pad, nitrocellulose membrane, waste pad to an adhesive backing card. Not only did the Nafion maintain good contact with the nitrocellulose membrane, but the added benefit in lamination was that evaporation of the sample was decreased so that the assays could be performed for longer times.

4.2 Characterizing the double-gate ICP device

The CVC for the double-gate design (schematically represented in Scheme 3a) is shown in Fig. 1a (red line). The slope of the

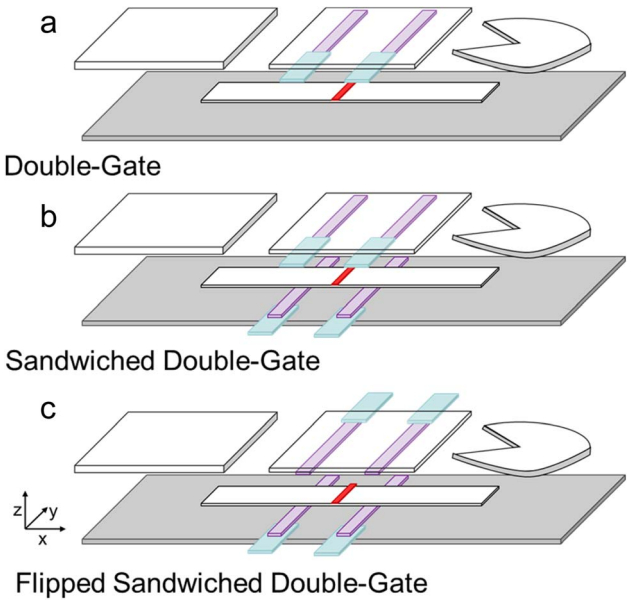

Scheme 3 Schematic of the three configurations of Nafion-coated electrodes – (a) double-gate, (b) sandwiched double-gate, and (c) flipped sandwich double-gate configurations.

CVC decreased at 10 V with the formation of the IDZ, which coincided with the onset of enrichment. Enrichment was improved as the voltage was increased. We hypothesized that we could improve the enrichment factor (EF), defined as the background subtracted fluorescence intensity of the region containing the enriched plug divided by the background subtracted fluorescence intensity of the wetted nitrocellulose membrane (taken before the voltage is turned on), by further improving the contact between the Nafion-coated electrodes and the nitrocellulose membrane and by decreasing the ionic resistance of the Nafion.

The device design was improved by sandwiching the nitrocellulose membrane with two sets of Nafion-coated electrodes, shown in Scheme 3b. The resistance of a substance is proportional to the length divided by the cross-sectional area. By sandwiching the nitrocellulose membrane with two Nafion membranes, the contact area was increased and therefore, the resistance of the system was decreased. The CVC for the sandwiched double-gate design is shown in Fig. 1a (blue line). The decreased electrical resistance of the Nafion-coated electrodes can be quantified by comparing the slopes of the of the ohmic region in the CVC for each configuration. The slope of the double-gate configuration is 9.0 $\mu A\ V^{-1}$, while the slope of the sandwiched double-gate configuration is 18.3 $\mu A\ V^{-1}$. Since the contact area was doubled, this increase in the slope by a factor of 2.03 is expected. In the ohmic region of the CVC, the slope is equal to the inverse of the resistance. Therefore, a steeper slope indicates a lower resistance, indicating that the sandwiched double-gate design is less resistive than the single-layer double gate design. The average fluorescence intensity of the enriched plug was higher in the sandwiched double-gate design than the single-layer design (Fig. 1b), with maximum EFs of 4 ± 1 and 2.1 ± 0.8, respectively. Additionally, the uniformity of the enriched plug in the *x*-direction (perpendicular to the nitrocellulose membrane), shown in Fig. 1c and d, is improved in the sandwiched double-gate design compared to the double-gate design.

4.3 Enriching S-protein in paper

After characterizing the device design with an anionic dye, we used S-protein as the analyte moving forward. S-protein was chosen as our analyte for detecting SARS-CoV-2 because it has an isoelectric point of 6.24,[30] meaning that S-protein has a negative charge at pH 7 and can be focused by ICP in our device. Although it has been shown that nucleocapsid protein (N-protein) can have a higher abundance per virus particle than S-protein,[31] the isoelectric point of nucleocapsid protein is 10.07,[30] meaning that N-protein would have a positive charge at biological pH, and would not focus *via* ICP in our device.

Pretreatment of the LFA was required to decrease non-specific adsorption between the charged protein and the nitrocellulose membrane. The pretreatment solution from Lee and co-workers (composed of 10 mM 2-amino-2-methyl-1-propanol (pH 9.0), 0.5% BSA, 0.5% β-lactose, 0.05% Triton X-100, 0.05% sodium azide)[32] as well as a commercially available LFA pretreatment solution, Stabilgaurd,[33] were first used. Both pretreatment solutions resulted in poor flow of the S-protein in the nitrocellulose membrane and minimal enrichment (see Fig. S3†). Pluronic is a triblock copolymer composed of hydrophilic tails and a hydrophobic center often used in polydimethylsiloxane (PDMS)-glass microfluidic devices to increase the hydrophilicity and decrease nonspecific adsorption of biomolecules to the PDMS surface.[34] Pretreatment of the nitrocellulose membrane and sample pads with 1.0 mM Pluronic F-127 solution yielded better flow of the protein in the nitrocellulose membrane and improved enrichment.

Unfortunately, the S-protein in the nitrocellulose membrane flowed slowly past the cathodic Nafion-coated electrode. We hypothesized that the low concentration and volume of Tris buffer (100 mM) did not have a sufficiently high buffering capacity to negate acidification of the adjacent segment of the nitrocellulose membrane by Nafion. Additionally, the location of the enriched plug was near the anodic Nafion-coated electrode, meaning that the test line would be slightly overlapping with the acidic Nafion. Binding of S-protein to ACE2 is pH dependent (see Fig. S4†), with the best binding occurring around pH 7 (see ESI† for evidence). For these reasons, we investigated alternative buffers for our ICP-enhanced LFA.

Two candidates were investigated: HEPES and Bis-Tris propane. Both buffers were chosen because they have two acidic protons and therefore larger buffering ranges. Additionally, both molecules are bulky and have lower conductivity than other biological buffers, which is important to minimize Joule heating and to prevent formation of gas bubbles by electrolysis at the electrodes. To obtain a biological pH for Bis-Tris propane, a high conductivity was obtained from the addition of acid. The enrichment was minimal and near the anodic Nafion-coated electrode because of the difficulty to deplete the high concentration of ions (see Fig. S5†). HEPES buffer was used in further

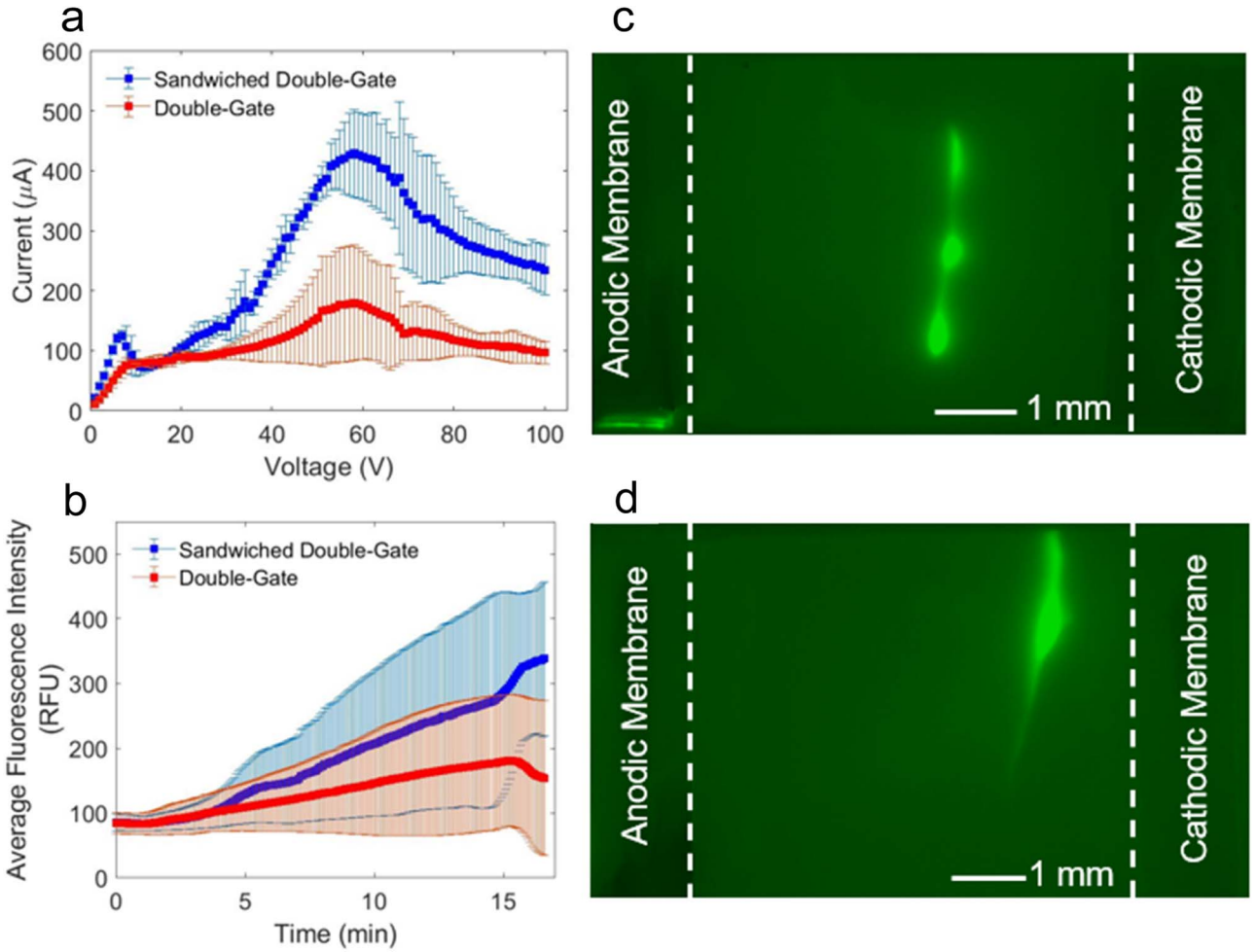

Fig. 1 The sandwiched double-gate (blue, c) and double-gate (red, d) configurations of Nafion-coated electrodes. Tris buffer is used as the running buffer and a green-fluorescent dye, $BODIPY^{2-}$ (50 nM), served as the focused analyte. (a) The current is measured as the voltage is ramped from 1.0 to 100.0 V with a rate of 1.0 V per 10 s. The current represents the average current obtained for each voltage applied. Error bars represent 1 standard deviation of the average current from 3 replicates. (b) The average fluorescence intensity of a rectangular region containing the enriched plug while the CVCs from (a) were collected. Error bars represent 1 standard deviation of the average fluorescence intensity from 3 replicates. (c and d) Fluorescence micrographs of the enriched plug at 100.0 V for the (c) sandwiched double-gate and (d) double-gate configurations.

experiments because its conductivity was low (2.0 mS cm^{-1}), and the focused plug of S-protein was not overlapping with the Nafion-coated electrodes. It's important to note that enrichment is demonstrated in "neat" buffer and would need to be adapted to clinical samples. While ICP has been successfully demonstrated in biofluids, such as urine[35] and blood,[36] the high ionic conductivity of biological samples is challenging to ICP focusing. Moreover, interfering proteins present in the sample co-enrich and can drive lower mobility targets, such as nucleic acids, upstream.[37] Reduction in non-specific binding can aid in preventing false positives that would be given by interfering proteins. We envision the ICP-enhanced LFA could be utilized for the analysis of patient nasal swabs, if a low salinity viral transport medium is prepared. Universal viral transport mediums are typically formulated with balanced salt solutions and can be buffered to an ideal pH with HEPES.[38] Future studies will determine the highest ionic strength compatible with the ICP-enhanced LFA in order to avoid dilution of samples prior to enrichment.

4.4 Improving the uniformity of enriched S-protein in the *x*-dimension

Interestingly, when the buffer was switched from Tris to HEPES, the CVCs reflected a change in resistance trends in the ohmic regions of the two configurations initially considered (double-gate and sandwiched double-gate, Fig. 1a yellow and red lines, respectively). In the sandwiched configurations, the ohmic regions of the CVC reflect a modest decrease in slope compared to the double-gate configuration instead of the 2-fold increase that was observed when Tris buffer was used. We believe this phenomenon is due to the change in conductivity between the two buffers. The conductivity of Tris buffer is 2.5 mS cm^{-1}, while the conductivity of HEPES buffer is 1.8 mS cm^{-1}. The ohmic region of the CVC should reflect the total resistance in

our device. If we consider our device as a circuit, we could model the anodic Nafion-coated electrode, the buffer-soaked nitrocellulose membrane, and the cathodic Nafion-coated electrode as three resistors in series. The resistance due to the buffer-soaked nitrocellulose membrane contributes a smaller proportion of the total resistance of the device when using Tris buffer than it does with HEPES because Tris buffer is more conductive than HEPES buffer. Therefore, in the Tris buffer CVCs, the resistance in the ohmic region is dictated by the resistance of the Nafion-coated electrodes. In the HEPES buffer CVCs, the resistance in the ohmic region is more controlled by the resistance of the buffer-soaked nitrocellulose membranes, so the slopes are both lower than those obtained for Tris and more similar to each other (1.12 μA V^{-1} for the sandwiched configuration and 1.59 μA V^{-1} for the double-gate configuration). The CVC begins to deviate from a linear slope at lower voltages for sandwiched configurations (13 V) than the double-gate configuration (22 V) as the IDZ grows, indicating that the sandwiched configurations still had a favorable effect on the onset voltage required for enrichment.

The flipped sandwich configuration (depicted in Scheme 3c) was chosen over the sandwiched configuration because the focused plug was more uniform in the *x*-direction (perpendicular to the nitrocellulose membrane), as demonstrated in Fig. 2c and d. This asymmetric focused plug occurs because the electric field is not uniform across the width of the nitrocellulose membrane due to the highly resistive nature of both the Nafion membranes and the nitrocellulose membrane. By flipping the top layer of Nafion-coated electrodes, we are applying the voltage at both the top and bottom edges of the nitrocellulose membrane, resulting in a more uniform electric field and focusing pattern.

As shown in Fig. 3a, the enriched plug consists of two spots of enrichment in a line perpendicular to the nitrocellulose

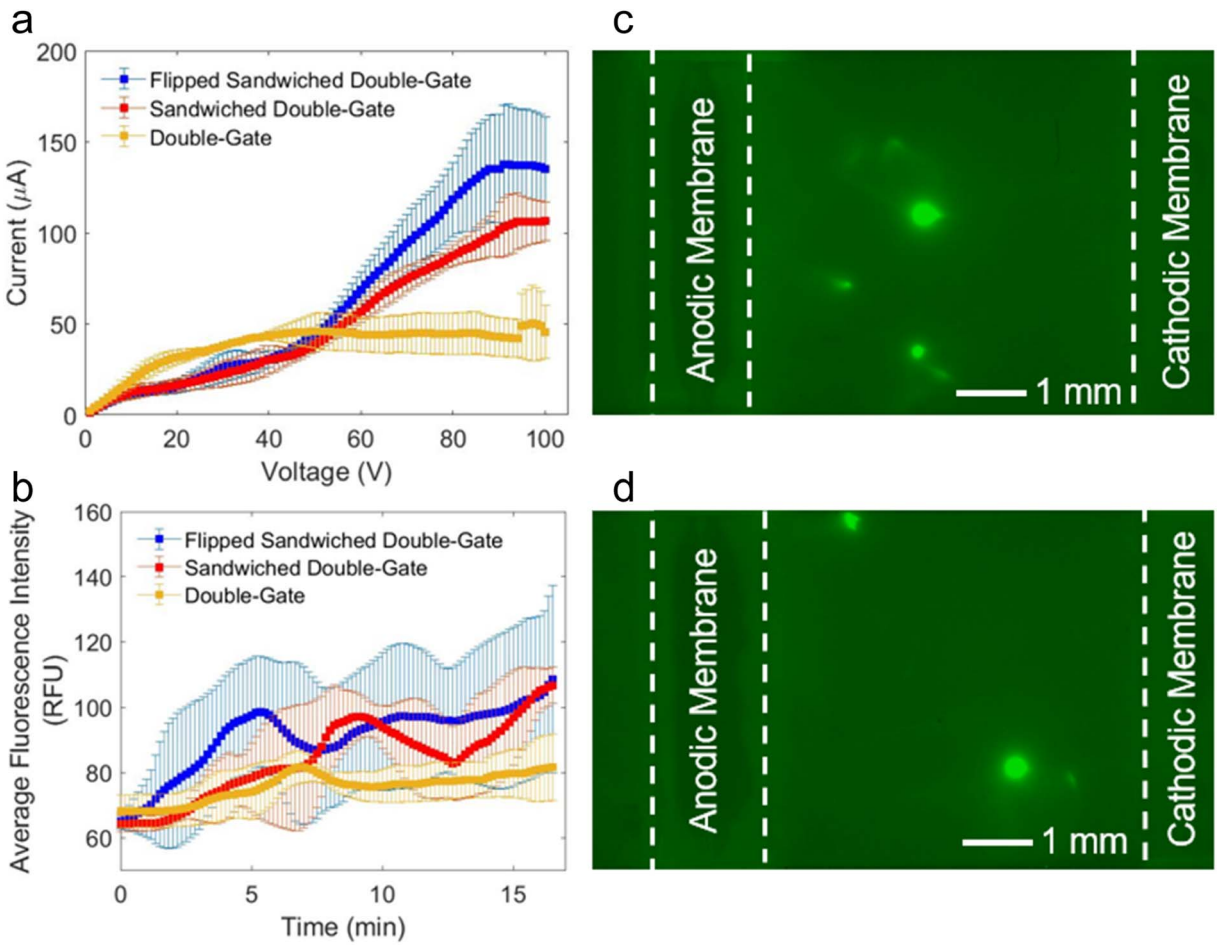

Fig. 2 The flipped sandwiched double-gate (blue, c) and sandwiched double-gate (red, d) and double-gate (yellow) configurations of Nafion-coated electrodes. HEPES is used as the running buffer and S-protein conjugated with a green dye (0.1 μg mL^{-1}), served as the focused analyte. A solution of 1.0 mM Pluronic F-127 was used to pretreat the nitrocellulose membrane and sample pad. (a) The current is measured as the voltage is ramped from 1.0 to 100.0 V with a rate of 1.0 V per 10 s. The current represents the average current obtained for each voltage applied. Error bars represent 1 standard deviation of the average current from 3 replicates. (b) The average fluorescence intensity of a rectangular region containing the enriched plug while the CVCs from (a) were collected. Error bars represent 1 standard deviation of the average fluorescence intensity from 3 replicates. (c and d) Fluorescence micrographs of the enriched plug at 100.0 V for the (c) flipped sandwiched double-gate and (d) sandwiched double-gate configurations.

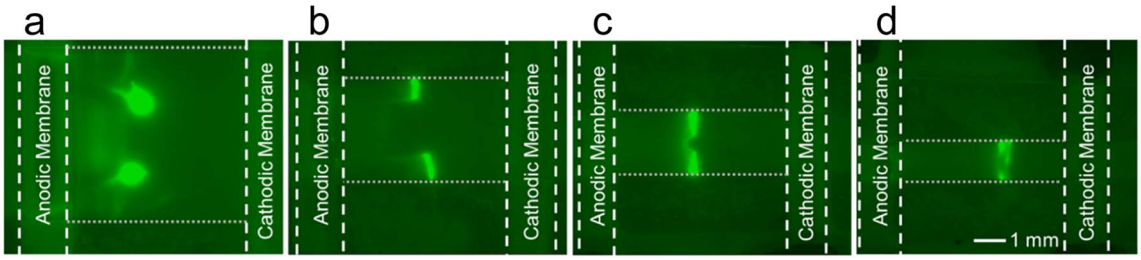

Fig. 3 Fluorescence micrographs of ICP experiments where the width of the nitrocellulose membrane is altered from 5.0 mm (a), to 3.0 mm (b), 2.0 mm (c), and 1.0 mm (d). The voltage was ramped from 1.0 V to 100.0 V with a rate of 1.0 V per 10 s, and these micrographs were taken at 100.0 V. In each trial, HEPES is used as the running buffer and S-protein conjugated with a green dye (0.4 μg mL^{-1}), served as the focused analyte. A solution of 1.0 mM Pluronic F-127 was used to pretreat the nitrocellulose membrane and sample pad.

membrane. To increase the uniformity of the enriched plug in the *y*-direction (parallel to the nitrocellulose membrane), the width of the nitrocellulose membrane was decreased from 5.0 mm (Fig. 3a) to 1.0 mm (Fig. 3d). The gap between the two enriched plugs decreased as the width decreased, until ultimately the focused plug formed a single band across the entire width of the nitrocellulose membrane.

From a CVC of the new configuration with a 1.0 mm-wide nitrocellulose membrane (Fig. S6†), HEPES buffer and the flipped-sandwich Nafion configuration, the onset voltage for ICP is maintained at 13 V. However, the change in width increased the resistance of the device, further decreasing the total current throughout the device. The maximum current in the CVC was attenuated from 140 ± 40 μA to 22 ± 3 μA, which is favorable for the adaptation of this device to point of care applications, because low power requirements (1.8 mW) can be powered by a battery-operated device.

4.5 Focusing S-protein over a test line in a LFA

After confirming the enrichment of S-protein in a nitrocellulose membrane, a test line composed of an ACE2 capture protein tagged with a red fluorescent dye was deposited on the nitrocellulose membrane.[32] The test line was aligned such that the plug of enriched analyte would focus directly over the test line. In a traditional LFA, a second biorecognition element would be added that has a transduction element to indicate binding of the antigen to the capture probes. In our assay, the transduction element in the green fluorescent dye that is conjugated to the antigen. The average fluorescence intensity of the S-protein over the test line was calculated 20 min after the voltage was turned off to ensure that only protein bound to the test line was counted, and not just protein that had been enriched over the test line. Fig. 4a shows the average fluorescence intensity over the test line for a LFA with ICP-enrichment and a LFA without ICP-enrichment. The background subtracted average fluorescence intensity of the test line was 153 RFU with ICP-enrichment, while the LFA without ICP-enrichment yielded an average fluorescence intensity of 121 RFU at 40 min. The maximum fluorescence intensity values for the same experiments at $t = 40$ min are 232 RFU with ICP-enrichment and 175 RFU without ICP-enrichment. Fluorescence intensities along a cut-line through the middle of the LFA are shown in Fig. 4b for three scenarios: during enrichment of the LFA (blue, corresponding the micrograph in Fig. 4c), after enrichment (red, corresponding to Fig. 4d), and for an LFA without enrichment (yellow). The vertical line denotes the front edge of the test line. Comparing the fluorescence intensities after enrichment and without enrichment, an increase in fluorescence intensity is observed along the test line. The fluorescence micrograph in Fig. 4c shows the LFA with ICP-enrichment. The red outline indicates the location of the test line. The focused plug of S-protein is well aligned with the location of the test line. After the voltage has been turned off, the portion of the enriched plug that has not bound to the test line flows downstream towards the waste pad. At $t = 40$ min (20 min after the voltage has been turned off), the fluorescence micrograph (Fig. 4d) has a brighter fluorescence intensity in the region where the S-protein had been enriched, indicating that some of the focused S-protein stayed bound to the ACE2 capture probes.

The signal enhancement (SE), defined as the average fluorescence intensity of the test line after the assay is complete divided by the average fluorescence intensity of the test line immediately after the test solution has wicked across the test line, of the LFA with ICP-enrichment at $t = 40$ min was 4.1, while the SE for the LFA without ICP-enrichment at $t = 40$ min was 1.3. Interestingly, the initial average fluorescence intensity of the nitrocellulose membrane just after the solution has wicked across the test line (*i.e.*, the denominator in the SE calculation) is lower for the LFA with Nafion-coated electrodes than without (37.6 RFU and 91.4 RFU, respectively). We hypothesize that this decrease in fluorescence intensity occurs because the acidic Nafion membranes still disrupt the flow of the S-protein across the strip. When reading a paper-based LFA, a positive result is determined by the user identifying the presence of a line. In the context of our LFA where the antigen is conjugated with a green-fluorescent dye, a green test line will be easier to see against a lower background intensity of the surrounding part of the nitrocellulose membrane. Therefore, we will compare the SE instead of the average fluorescence intensity of the test line when comparing the performance of the LFA configurations.

Recent studies have demonstrated that the net charge of S-protein changes with different variants of SARS-CoV-2.[39] A change in the charge of a molecule will result in a change in

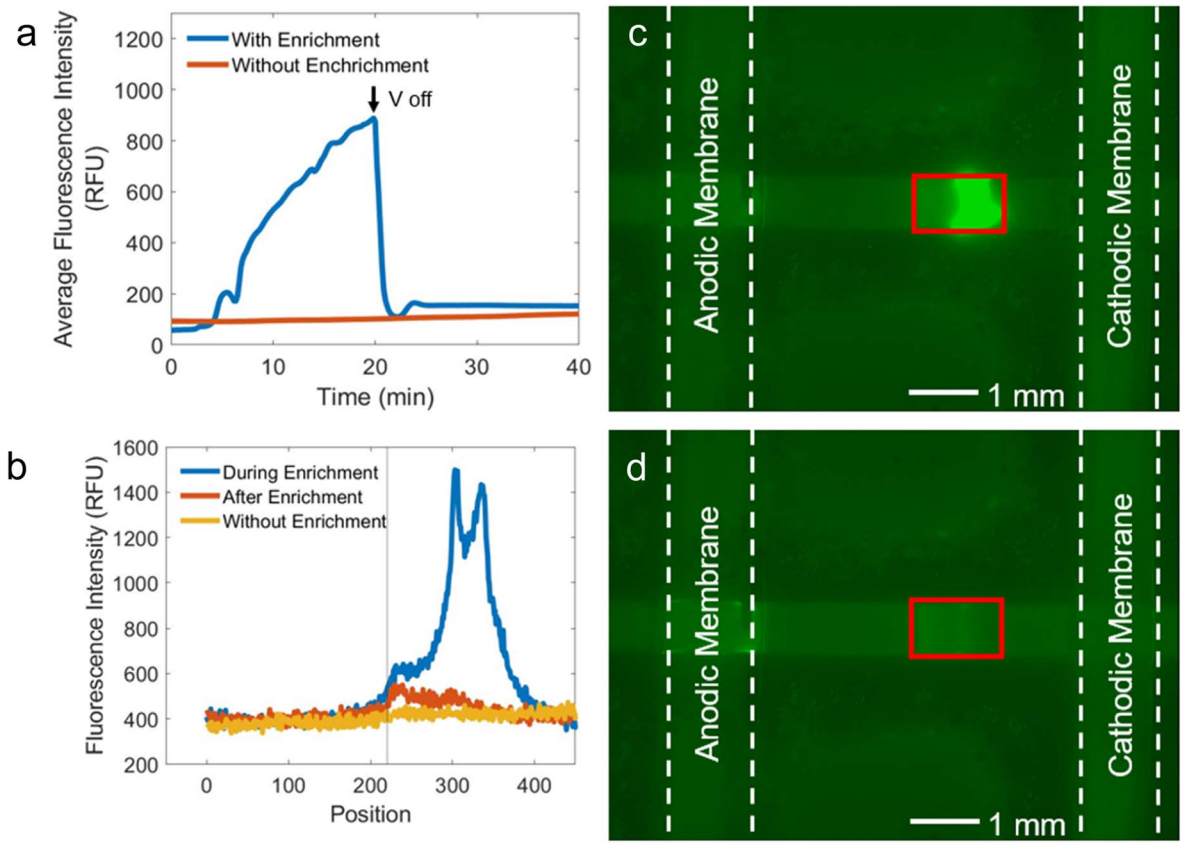

Fig. 4 (a) The average fluorescence intensity of the region containing the test line during a LFA with enrichment (blue) and an LFA without enrichment (red). In the LFA with enrichment, the voltage is ramped from 1.0 to 80.0 V at a rate of 1.0 V per 10 s, then the voltage is held at 80.0 V for a total of 20 min. The black arrow indicates when the voltage is turned off. The time has been adjusted such that $t = 0$ when the solution has already wicked across the nitrocellulose membrane. In these experiments, the nitrocellulose membrane has been modified with ACE2 capture probes as a test line. HEPES is used as the running buffer and S-protein conjugated with a green dye (0.4 μg mL^{-1}), served as the focused analyte. A solution of 1.0 mM Pluronic F-127 was used to pretreat the nitrocellulose membrane and sample pad. (b) The fluorescence intensity from a cut-line along the middle of the LFA during enrichment (blue), after enrichment (red), and for an LFA without enrichment (yellow). The vertical line indicates the beginning location of the test line. (c) A fluorescence micrograph of the LFA with enhancement at $t = 20$ min (80.0 V applied). The red box indicates the position of the test line. (d) A fluorescence micrograph of the LFA from (c) at $t = 40$ min.

electrophoretic mobility, which may alter the axial position where the molecule is focused. This property may alter the location that the test line should be aligned because the analyte may focus in a different location. However, we believe that the change in focusing location will be minimal for the variants of S-protein because the percent change in the charge of the protein is small; according to Pawłowski, the formal charge of wild-type S-protein is -12 elementary charge units (e) and mutations have resulted in a net change to the formal charge of S-protein by -1, 0, 1, or $2e$.[39] Others report that the net charge of the surface of the folded S-protein is $-32e$.[40]

4.6 Improving the reproducibility of the focused plug location in a LFA

In previous examples of paper-based ICP-enhanced devices, a direct voltage that is higher than the voltage required for onset of ICP is applied to the device to focus the analyte.[15,17,19,20] However, it was found that the direct application of a high voltage resulted in enrichment that occurred in irreproducible locations between the two Nafion-coated electrodes. In this context, a reproducible enrichment location is required because the test line is aligned directly under this location. We found that by ramping the voltage at a rate of 1.0 V per 10 s, the location of the enriched plug was reproducible due to a slower formation of the IDZ in the nitrocellulose membrane. For example, for the experiments in Fig. 5, only 3 trials were required to collect triplicate data for the ramped voltage case, while 6 trials were required to collect 3 trials where the enriched plug overlapped with the test line when the voltage was applied as direct voltage. Further studies are required to understand why ramping the voltage leads to more reproducible enrichment plug locations than directly applying a high voltage.

Fig. 5 shows the average fluorescence intensity of the test line over time for two cases; one where 80 V was directly applied to the Nafion-coated electrodes, and one where the voltage is ramped to 80 V at a rate of 1.0 V per 10 s ($n = 3$). The voltage is applied for 20 min in each case. The average maximum fluorescence intensity is slightly higher for the ramped case, as shown in Fig. 5a, but more importantly the standard deviation

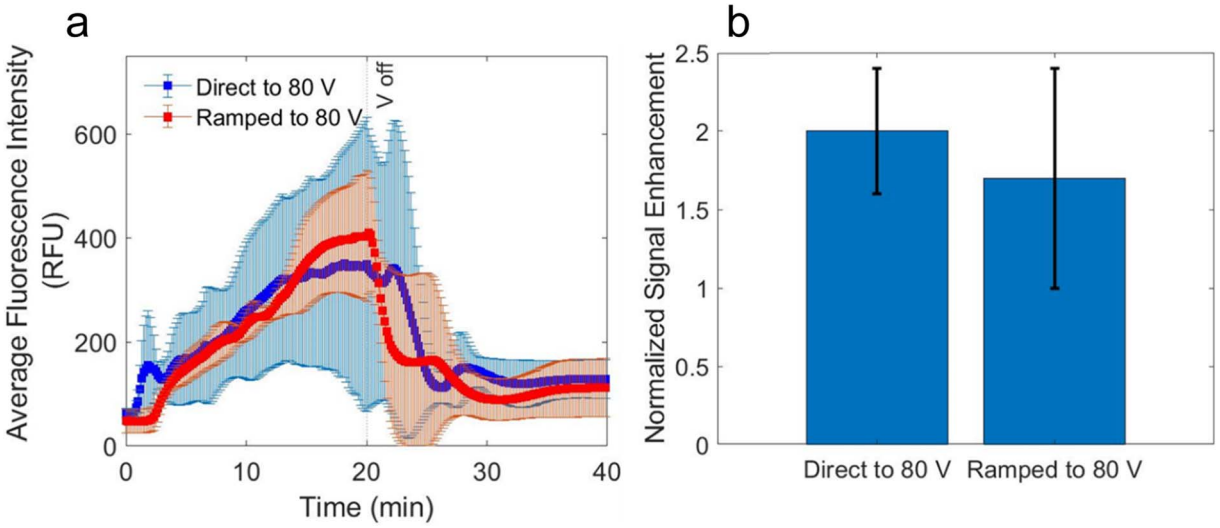

Fig. 5 (a) The average fluorescence intensity of the region containing the test line during a LFA with enrichment where 80.0 V is directly applied (blue) and where the voltage is ramped from 1.0 to 80.0 V at a rate of 1.0 V per 10 s (red). In both cases, the voltage is turned off after 20 min, indicated by a dashed line. In these experiments, the nitrocellulose membrane has been modified with ACE2 capture probes as a test line. HEPES is used as the running buffer and S-protein conjugated with a green dye (0.4 μg mL^{-1}), served as the analyte. A solution of 1.0 mM Pluronic F-127 was used to pretreat the nitrocellulose membrane and sample pad. Error bars represent 1 standard deviation of the average fluorescence intensity from 3 replicates where the enriched plug was aligned with the test line. (b) The average nSE of the test line at $t = 40$ min for each voltage condition. The error bars represent 1 standard deviation of the nSE from 3 replicates.

of the fluorescence intensity between each trial (indicated by error bars in Fig. 5a) was lower for the ramped case than the direct voltage application case. By comparing the fluorescence intensity of the enriched plug to a calibration curve of fluorescence intensities of distinct protein concentrations (0.1 to 100 μg mL^{-1}) in the nitrocellulose membrane (Fig. S7†), the enriched concentration could be calculated. It was found that the enriched plug was 16.7-fold higher than the initial concentration added for the ramped voltage case, and 14.3-fold higher for the direct voltage case.

The SE of the region of the nitrocellulose membrane containing the test line 20 min after the voltage had been turned off in an ICP-enhance LFA is plotted in Fig. 5b for the two voltage application methods. To account for day-to-day variability of the test line, the SE is normalized (nSE) by the SE of an LFA without ICP-enhancement taken on the same day. Therefore, an nSE of 1.0 would indicate that the ICP-enhanced LFA yielded the same SE as an LFA without ICP-enhancement. The average nSE for the direct voltage case was 2.0 ± 0.4, while for the ramping case the enhancement was 1.7 ± 0.7, which are not significantly different ($p = 0.33$). The lack of reproducibility of the location of the enriched plug led us to the conclusion that ramping the voltage in an ICP-enhanced LFA is more favorable.

4.7 Optimizing the binding of enriched S-protein to the test line

After determining the best configuration for ICP-enhancement of an LFA, the maximum voltage and time of voltage application was optimized. First, three voltages were investigated for enrichment: 20 V, 50 V, and 80 V. These three voltages were chosen because they occur at points in the CVC where the current is limiting, indicating that fewer vortices are allowing mixing of the IDZ and IEZ (and disrupting the stability of the focused analyte plug). Fig. 6a shows the average intensity of the test line over time while the voltage is applied. In each case, the voltage is ramped to the maximum voltage at a rate of 1.0 V per 10 s and then held at the maximum voltage for a total time of 20 min. The 80 V application showed the highest average fluorescence intensity over the test line. The 80 V case had a maximum of 28.9-fold increase in concentration during enrichment, while the 50 V and 20 V cases had EFs of 19.3- and 12.8-fold, respectively. Additionally, the improvement to the nSE of the test line after the voltage was turned off, shown in Fig. 6b, was highest for the 80 V case at 2.5-fold higher than a LFA without enrichment, followed by 2.0 for 50 V and 1.6 for 20 V. The values for 80 V and 20 V were significantly different ($p = 0.03$), however the values for 50 V and 20 V were not significantly different ($p = 0.07$), therefore 80 V was determined as the best voltage for enhancing the LFA with ICP.

After determining the optimal voltage for ICP-enrichment, the optimal time for enrichment was investigated. Fig. 6c shows the average fluorescence intensity over the region containing the test line over time for this investigation. In each case, the voltage was ramped to 80 V at a rate of 1.0 V per 10 s and then held at the maximum voltage for a total time of 15 min, 20 min, or 30 min. Notably, the scale for the average fluorescence intensity in Fig. 6c is lower by a factor of 4 than the scale for Fig. 6a. This change is because the initial concentration of S-protein in our sample solution was decreased by a factor of 4. It was found that 20 min and 30 min yielded statistically similar improvements ($p = 0.5$) to average fluorescence intensity of the test line after voltage application, shown

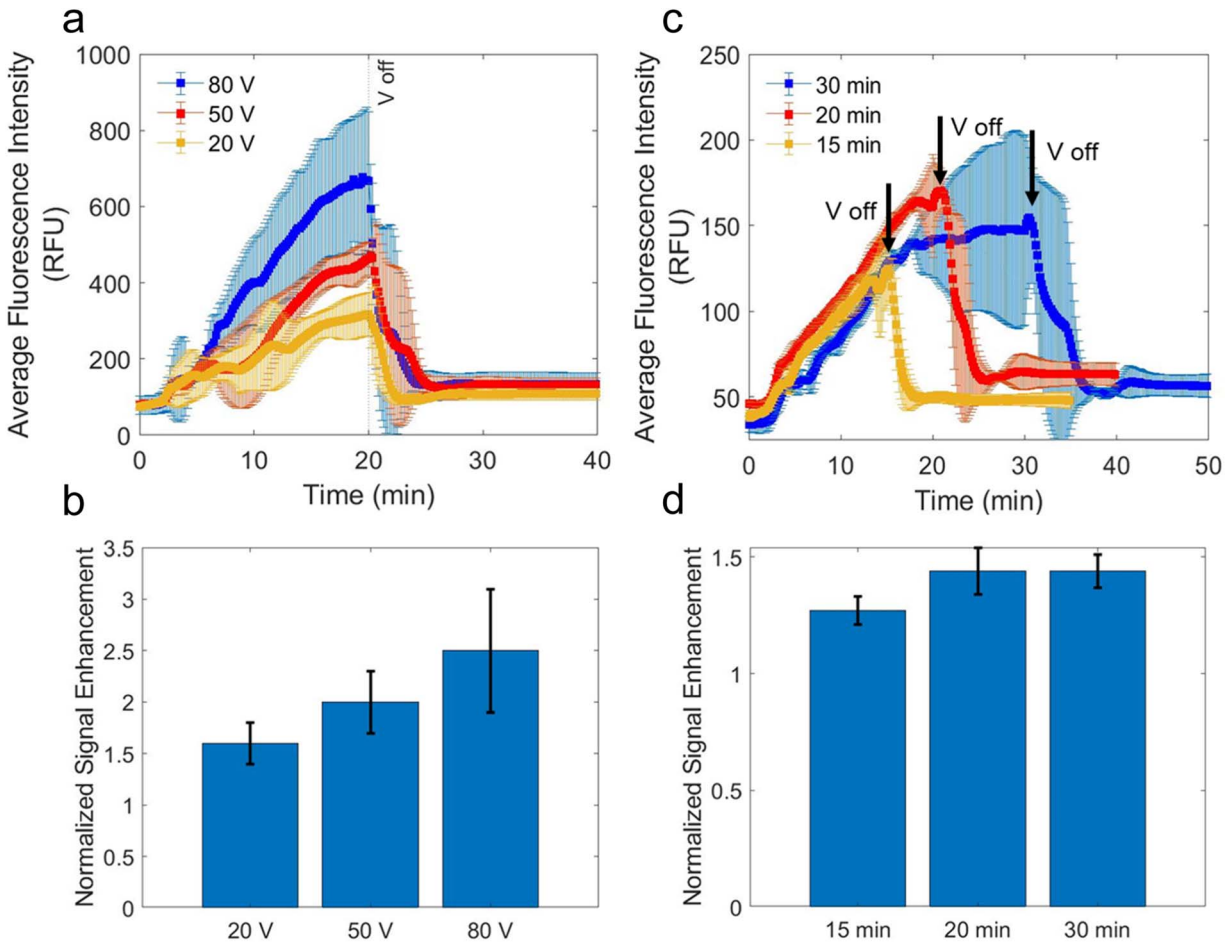

Fig. 6 In these experiments, the nitrocellulose membrane has been modified with ACE2 capture probes as a test line. HEPES is used as the running buffer and S-protein conjugated with a green dye (0.4 μg mL^{-1}), served as the analyte. A solution of 1.0 mM Pluronic F-127 was used to pretreat the nitrocellulose membrane and sample pad. Error bars represent 1 standard deviation of the average fluorescence intensity from 3 replicates. (a) The average fluorescence intensity of the region containing the test line during a LFA with enrichment where the voltage is ramped from 1.0 to 80.0 V (blue), 50.0 V (red), or 20.0 V (yellow) at a rate of 1.0 V per 10 s. In each case, the voltage is turned off after 20 min, indicated by a dashed line. (b and d) The average nSE of the test line at $t = 40$ min for each voltage condition from (a) and (c), respectively. The error bars represent 1 standard deviation of the average nSE from 3 replicates. (c) The average fluorescence intensity of the region containing the test line during an LFA with enrichment where the voltage was ramped from 1.0 to 80.0 V at a rate of 1.0 V per 10 s for a total time of 30 min (blue), 20 min (red) or 15 min (yellow). The black arrows indicate the time when voltage is turned off.

in Fig. 6d, likely because we had reached saturation conditions. Both enrichment times yielded significantly improved enrichment than the 15 min enrichment time ($p = 0.03$ for 20 min and $p = 0.01$ for 30 min). Therefore, 20 min was chosen as the optimal enrichment time because for a POC device, a faster test is more favorable.

4.8 Increasing the sensitivity of a LFA with ICP-enrichment

The best conditions for a LFA with ICP-enrichment were determined to be a HEPES running buffer, the flipped-sandwich Nafion coated electrodes, a 1 mm-wide nitrocellulose membrane pretreated with 1.0 mM Pluronic solution. The optimal voltage application method was ramping to 80.0 V for a total of 20 min voltage application.

The improvement to the sensitivity of the LFA with ICP-enrichment compared to the LFA without ICP-enrichment was calculated by dividing the slope of the linear portion of the calibration curve with enrichment by the slope of the linear portion of the calibration curve without enrichment, shown in Fig. 7. We found that the ICP-enriched LFA yielded a 2.9 ± 0.5-fold higher signal than the LFA without enrichment. On average, there was a 21 ± 4-fold increase in concentration of S-protein over the test line during enrichment. Using eqn (1), the expected improvement of the amount of S-protein that binds to the test line with an increased concentration of S-protein can be calculated by comparing the limit of the amount bound to the test line (h_{lfa}), which is equal to $\frac{C_0^*}{1 + C_0^*}$. For example, the maximum increase in concentration for the ICP-enhanced LFA with 0.4 μg mL^{-1} S-protein was 21-fold; this increase in concentration should have led to a 16-fold increase in the amount of S-protein bound to the test line. However, only a 1.6-fold increase was observed.

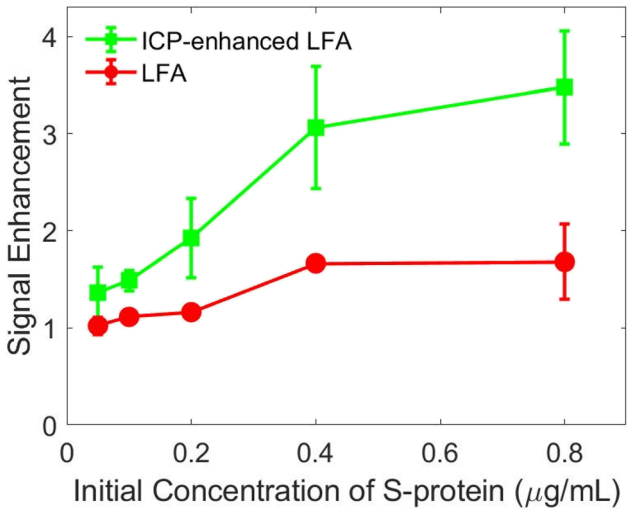

Fig. 7 A calibration curve comparing the signal enhancement of the region containing the test line at $t = 40$ min for five initial concentrations of S-protein for an LFA with enrichment (blue) and an LFA without enrichment (red). For the LFA with enrichment, the voltage was ramped from 1.0 to 80.0 V at a rate of 1.0 V per 10 s for a total time of 30 min. The error bars represent 1 standard deviation of the signal enhancement from 3 replicates.

We hypothesize that the improvement to the amount of S-protein bound to the test line is not as high as expected for several reasons. First, the enriched plug does not cover the entire test line area, but we report the average fluorescence intensity of the entire test line area. For example, in one LFA with ICP-enrichment the average SE for the total area of the test line was 2.3, while the average SE for a smaller portion of the test line where S-protein was focused was 4.3. Second, we are using dissociation constant measurements from Lee and co-workers;[32] the kinetics are likely different in our assay because both the S-protein and the ACE2 capture probes are conjugated to dyes. If the dissociation constant is in fact lower by a factor of 90, for example, then the expected improvement of the amount of S-protein that binds to the test line following 21-fold enrichment is only 1.6-fold (not 16-fold), indicating that the binding kinetics could be better than what is reported by Lee and co-workers. Third, after enrichment, the voltage is turned off and the test line is exposed to sample solution that does not have as high a concentration of S-protein as the enriched plug. In other words, before we measure the SE, we allow the enriched plug to wash off of the test line so that S-protein that is not bound is not counted in our measurement. Because the amount of the S-protein that is bound to the test line is in equilibrium with the unbound S-protein, we may be losing protein that was bound during enrichment during this wash period. Lastly, it is possible that the protein structures have been altered or denatured due to a change in temperature from Joule heating, and pH and salt concentration between the Nafion membranes, which can decrease the binding affinity. Incorporation of the previously reported paper stacks between the Nafion and LFA[23] may help to address this issue, while preserving our disposable membrane-coated electrode design that is most suited to the POC. We hope to answer these questions with future studies in our lab.

5. Conclusion

In this paper, we described the enhancement of a LFA by incorporating ICP-enrichment to focus the antigen directly over the capture probes. The running buffer and pretreatment solution were investigated to find compositions that were biocompatible and could be used with ICP-enrichment. HEPES buffer and a Pluronic solution were identified as amenable solutions because of their low conductivity and the buffering range of HEPES. Configurations for incorporating Nafion-coated electrodes in a LFA were investigated and optimized for highest SE and lowest power requirements. The flipped sandwiched double-gate configuration where both layers of Nafion-coated electrodes were adhesive was found to be the optimal configuration. The method of voltage application for preconcentration and the width of the nitrocellulose membrane were optimized to create a reproducible location for the enriched plug that spanned the width of the test line. Ramping the voltage to the desired voltage was found to create a static focusing location, and the 1.0 mm-wide nitrocellulose membrane had the most uniform enriched plug across the width of the test line. A maximum enrichment voltage of 80 V for a total application time of 20 min yielded the highest improvement to the amount of antigen that bound to the test line. Finally, the described ICP-enhanced LFA was found to be 2.9-fold more sensitive than a LFA without enhancement, indicating that a lower concentration of antigen can be detected with the modified LFA, which should lead to earlier diagnosis times for COVID-19 patients.

Future improvements to this ICP-enhanced LFA include the addition of a detector antibody conjugated with a Au NP so that the LFA can be read by eye or a with a camera instead of requiring fluorescence detection. Additionally, the device design will be modified further to increase the electric field strength in the region containing the capture probes and therefore improve the enrichment of the antigen to improve binding to the capture probes. Ultimately, we aim to improve the sensitivity of the ICP-enhanced LFA and the amenability of the proposed platform for POC applications.

Conflicts of interest

There are no conflicts to declare.

Acknowledgements

The authors gratefully acknowledge funding through the Research Corporation for Scientific Advancement COVID Initiative and the Roy J. Carver Charitable Trust. The authors would also like to thank Dr Evan T. Camrud for his consultation in mathematics.

References

1 Y. Liu, L. Zhan, Z. Qin, J. Sackrison and J. C. Bischof, *ACS Nano*, 2021, **15**, 3593–3611.
2 M. Peña-Rodríguez, O. Viera-Segura, M. García-Chagollán, J. S. Zepeda-Nuño, J. F. Muñoz-Valle, J. Mora-Mora,

G. Espinoza-De León, G. Bustillo-Armendáriz, F. García-Cedillo and N. Vega-Magaña, *J. Clin. Lab. Anal.*, 2021, **35**(5), e23745.
3 F. Mahmoudinobar, D. Britton and J. K. Montclare, *Protein Eng., Des. Sel.*, 2021, **34**, 1–10.
4 W. W.-W. Hsiao, T.-N. Le, D. M. Pham, H.-H. Ko, H.-C. Chang, C.-C. Lee, N. Sharma, C.-K. Lee and W.-H. Chiang, *Biosensors*, 2021, **11**, 295.
5 V. Shirshahi and G. Liu, *TrAC, Trends Anal. Chem.*, 2021, **136**, 116200.
6 S. Kasetsirikul, M. J. A. Shiddiky and N. T. Nguyen, *Microfluid. Nanofluid.*, 2020, 24.
7 J. D. Bishop, H. v. Hsieh, D. J. Gasperino and B. H. Weigl, *Lab Chip*, 2019, **19**, 2486–2499.
8 B. Y. Moghadam, K. T. Connelly and J. D. Posner, *Anal. Chem.*, 2015, **87**, 1009–1017.
9 A. Sharma, A. I. Y. Tok, C. Lee, R. Ganapathy, P. Alagappan and B. Liedberg, *Sens. Actuators, B*, 2019, **285**, 431–437.
10 F. Mashayekhi, A. M. Le, P. M. Nafisi, B. M. Wu and D. T. Kamei, *Anal. Bioanal. Chem.*, 2012, **404**, 2057–2066.
11 A. Drexelius, A. Hoellrich, A. Jajack, E. Gomez, M. Brothers, S. Hussain, S. Kim and J. Heikenfeld, *Biomicrofluidics*, 2020, **14**(5), 054101.
12 M. Li and R. K. Anand, *Analyst*, 2016, **141**, 3496–3510.
13 B. Berzina and R. K. Anand, *Anal. Chim. Acta*, 2020, **1128**, 149–173.
14 A. Krishnamurthy and R. K. Anand, *TrAC, Trends Anal. Chem.*, 2022, **148**, 116537.
15 S. il Han, K. S. Hwang, R. Kwak and J. H. Lee, *Lab Chip*, 2016, **16**, 2219–2227.
16 A. T. K. Perera, S. Pudasaini, S. S. U. Ahmed, D. T. Phan, Y. Liu and C. Yang, *Electrophoresis*, 2020, **41**, 867–874.
17 C. Kim, Y. K. Yoo, S. il Han, J. Lee, D. Lee, K. Lee, K. S. Hwang, K. H. Lee, S. Chung and J. H. Lee, *Lab Chip*, 2017, **17**, 2451–2458.
18 K. Lee, Y. K. Yoo, S. il Han, J. Lee, D. Lee, C. Kim and J. H. Lee, *Micro Nano Syst. Lett.*, 2017, **5**, 11.
19 S. H. Yeh, K. H. Chou and R. J. Yang, *Lab Chip*, 2016, **16**, 925–931.
20 R. J. Yang, H. H. Pu and H. L. Wang, *Biomicrofluidics*, 2015, **9**(1), 014122.
21 X. Li, L. Luo and R. M. Crooks, *Anal. Chem.*, 2017, **89**, 4294–4300.
22 R. Kwak, J. Y. Kang and T. S. Kim, *Anal. Chem.*, 2016, **88**, 988–996.
23 C. Kim, Y. K. Yoo, N. E. Lee, J. Lee, K. H. Kim, S. Lee, J. Kim, S. J. Park, D. Lee, S. W. Lee, K. S. Hwang, S. Il Han, D. Lee, D. S. Yoon and J. H. Lee, *Biosens. Bioelectron.*, 2022, **212**, 114385.
24 K. H. Kim, Y. K. Yoo, N. E. Lee, J. Lee, C. Kim, S. Lee, J. Kim, S. J. Park, D. Lee, S. W. Lee, H. Kim, D. Hur, D. S. Yoon and J. H. Lee, *BioChip J.*, 2023, **17**, 340–348.
25 C. M. Han, E. Katilius and J. G. Santiago, *Lab Chip*, 2014, **14**, 2958–2967.
26 T. M. Squires, R. J. Messinger and S. R. Manalis, *Nat. Biotechnol.*, 2008, **26**, 417–426.
27 S. Mendez, E. M. Fenton, G. R. Gallegos, D. N. Petsev, S. S. Sibbett, H. A. Stone, Y. Zhang and G. P. López, *Langmuir*, 2010, **26**, 1380–1385.
28 N. Craig, S. L. Fletcher, A. Daniels, C. Newman, M. O'shea, W. S. Tan, A. Warr and C. Tait-Burkard, *Viruses*, 2022, **14**(3), 508.
29 High Containment Microbiology, NIS Laboratories, National Infection Service, Public Health England N.B., *SARS-CoV-2 inactivation: interim report*, 2020, HCM/CoV2/022/v1.
30 C. Scheller, F. Krebs, R. Minkner, I. Astner, M. Gil-Moles and H. Wätzig, *Electrophoresis*, 2020, **41**, 1137–1151.
31 P. D. Burbelo, F. X. Riedo, C. Morishima, S. Rawlings, D. Smith, S. Das, J. R. Strich, D. S. Chertow, R. T. Davey and J. I. Cohen, *J. Infect. Dis.*, 2020, **222**, 206–213.
32 J.-H. Lee, M. Choi, Y. Jung, S. K. Lee, C.-S. Lee, J. Kim, J. Kim, N. H. Kim, B.-T. Kim and H. G. Kim, *Biosens. Bioelectron.*, 2021, **171**, 112715.
33 E. Noviana, S. Jain, J. Hofstetter, B. J. Geiss, D. S. Dandy and C. S. Henry, *Anal. Bioanal. Chem.*, 2020, **412**, 3051–3061.
34 J. C. Wang, W. Liu, Q. Tu, C. Ma, L. Zhao, Y. Wang, J. Ouyang, L. Pang and J. Wang, *Analyst*, 2015, **140**, 827–836.
35 H. Gao, J. J. Liu, Y. Q. Liu and Z. Y. Wu, *Microfluid. Nanofluid.*, 2019, **23**, 51.
36 B. Berzina and R. K. Anand, *Anal. Chem.*, 2018, **90**, 3720–3726.
37 B. Berzina and R. K. Anand, *Anal. Chim. Acta*, 2020, **1128**, 149–173.
38 P. D. Kirkland and M. J. Frost, *Pathology*, 2020, **52**, 811–814.
39 P. H. Pawłowski, *Infect. Drug Resist.*, 2021, **14**, 5099–5105.
40 L. Casalino, Z. Gaieb, J. A. Goldsmith, C. K. Hjorth, A. C. Dommer, A. M. Harbison, C. A. Fogarty, E. P. Barros, B. C. Taylor, J. S. Mclellan, E. Fadda and R. E. Amaro, *ACS Cent. Sci.*, 2020, **6**, 1722–1734.

